SIMULATION AND EXPERIMENTAL STUDY OF BURIED NATURAL GAS PIPE-LINE LEAK DETECTION BASED ON SOUND SOURCE CHARACTERISTICS

by

Ting LIN[a], Zhichi WANG[b], Bin HU[c], Yubo JI[d], and Xiaoyu LIANG[a*]

[a] College of Metrology and Measurement Engineering, China Jiliang University, Hangzhou, China
[b] Hangzhou Qianjiang Gas Co., Ltd., Hangzhou, China
[c] China Special Equipment Inspection and Research Institute, Beijing, China
[d] Ningbo China Resources Xingguang Gas Co., Ltd., Ningbo, China

Original scientific paper
https://doi.org/10.2298/TSCI230313102L

Buried pipe-line leakage will affect the thermal characteristics of the soil environment, leading to a poor soil environment. In addition, leakage of natural gas possibly produces an explosion and subsequent fire, which has fatal harm. Sustainable detection of underground gas pipe-line leaks is a significant part of current research. In this study, a method for leak detection of buried natural gas polyethylene pipe-lines based on sound source characteristics is investigated. The simulation software was applied in analyzing the variation of leakage rate and sound source in buried pipes under different leakage conditions including mainly different leakage apertures and pipe pressures. Also, an experiment platform was built to verify the simulation results. These results can provide help for gas pipe-line leakage detection and safety protection.

Key words: *gas pipe-lines, leakage detection, sound source characteristics, numerical simulation, fluid mechanics*

Introduction

With the popularity of natural gas use and the rapid development of underground pipe-lines, natural gas leaks have become a major cause of gas pipe-line safety accidents. After leakage, a large amount of heating medium enters the soil, affecting the thermal characteristics of the soil environment, temperature, and humidity distribution, which will lead to a poor soil environment, deterioration of the heat transfer performance, and even system failure [1, 2]. In addition, leakage of natural gas into the air environment possibly produces an explosion and subsequent fire [3], which has fatal harm to people's life. When a pipe-line is leaking physical parameters such as gas density, pressure, flow rate, temperature, and acoustic field at and near the leak point change. By examining the medium flow and diffusion characteristics, the relationship between pipe-line parameters and medium leakage, and measuring the changes in these parameters will possibly identify, detect and locate leaks. Thus, analyzing the leakage state facilitates the detection of a pipe-line leakage accident.

Current commonly used leak detection methods include the negative pressure wave method, distributed fiber optic method, radioactive leak detection method, mass/volume balance method, air-borne laser and radar inspection technology, and acoustic wave method.

* Corresponding author, e-mail: xyliang@cjlu.edu.cn

Among them, the acoustic principle technology is often used for its high sensitivity, low false detection rate, and real-time accuracy when conducting research [4]. Already known that the leakage detection and location were greatly influenced by the working pressure and the leakage orifice diameter, leak noise is mainly concentrated at low frequencies (0-100 Hz), and the frequency spectrum of the signals can be used as the leakage detection characteristics [5-7]. In recent years, CFD simulations have become an essential tool for investigating pipe-line flows and leaks due to advances in the field of high speed computing, where software such as ANSYS, FLUENT, and COMSOL are frequently used [8, 9].

The thermal interaction between the ambient and subsurface objects is affected by the soil temperature distribution, and the effect of a buried pipe leakage on the soil environment must be considered. It will lead to excessive changes in soil temperature, reduce the performance of experimental instruments, and destroy the ecological environment. In addition, flow velocity, temperature, and the pipe-line under different buried depth factors have a great influence on the temperature change in the pipe, and the influence should be fully considered in pipe-line construction [10-12].

We found that most of the current research is focused on acoustic signal processing, or positioning algorithms, and relatively little research has been done on the basic characteristics and change laws presented by the pneumatic noise sound source during leakages, besides most of the research objects are steel pipes, and not much attention has been paid to non-metallic polyethylene material. Steel pipes and polyethylene pipes differ significantly in terms of elastic modulus, thermal conductivity, and other performance parameters, thus the acoustic properties exhibited during leakage and the change in the law of the pneumatic noise sound source presented are bound to differ. There are few studies on the sound source characteristics of polyethylene natural gas pipe-line leaks, so it is necessary to conduct a study. In this paper, ANSYS FLUENT was employed for simulating and analyzing the fluid-flow process and performance of the system under different leakage conditions, determining the effects of leak hole sizes and pipe-line pressure on flow rate and sound source characteristic parameters of the buried polyethylene pipe-line. Besides, an experimental platform was developed to compare and validate the numerical simulation.

Modelling and simulation methods

Mathematical models and principles

When a leak occurs, gas is ejected from the leak at a high velocity under the action of the internal and external pressure difference and interacts with the pipe wall and the external medium (soil) to produce a leak acoustic wave, thus the sound field and sound source characteristics at the leak hole will change. According to the changes and characteristics of the leakage process, the small hole leakage model is often applied to buried pipe-lines with a leakage aperture of less than 20 mm [13].

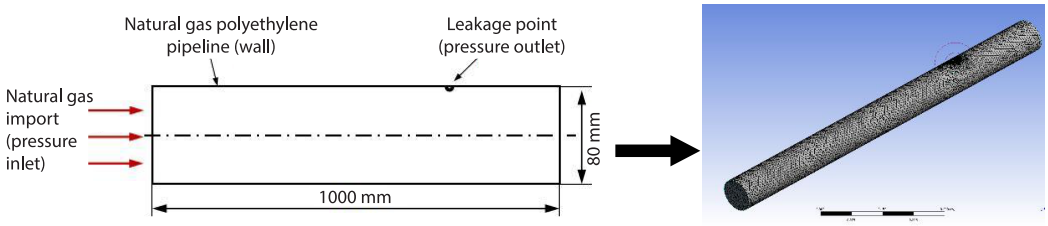

Figure 1. Physical model of leakage of a natural gas polyethylene pipe-line

The leak hole was located at the top of the pipe, the leakage direction was vertical ground upward, and the hole plane was parallel to the pipe axis. The pipe material was polyethylene, the pipe diameter 80 mm, the pipe wall thickness 5 mm, and the pipe length 1000 mm, as shown in fig. 1. The boundary condition of the pipe inlet was pressure inlet and pipe outlet, and the leakage hole was pressure outlet, the rest of the surface was set as the pipe wall surface. The ANSYS WORKBENCH was used to develop the geometric model and divided it into the generated mesh using the MESH module.

The grid division will directly affect the calculation speed and the accuracy of the results, therefore, the grid near the leakage hole was encrypted.

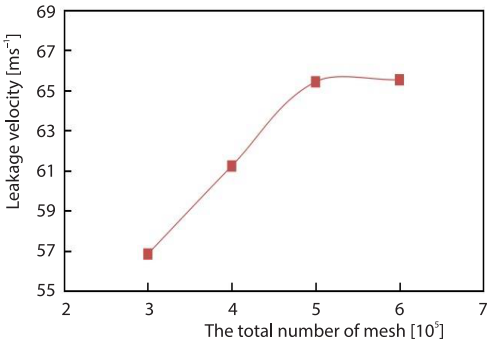

Figure 2. Grid-independence verification

To verify the grid independence, the simulation results of $3 \cdot 10^5$, $4 \cdot 10^5$, $5 \cdot 10^5$, and $6 \cdot 10^5$ were compared by dividing the computational domain into different numbers of grids. It can be found in fig. 2 that there is no significant change in the leakage velocity after the grid number exceeds $5 \cdot 10^5$, which is considered to meet the calculation accuracy requirements, indicating that the grid number is irrelevant to the calculation results at this time. Therefore, the number of meshes is chosen as 541326.

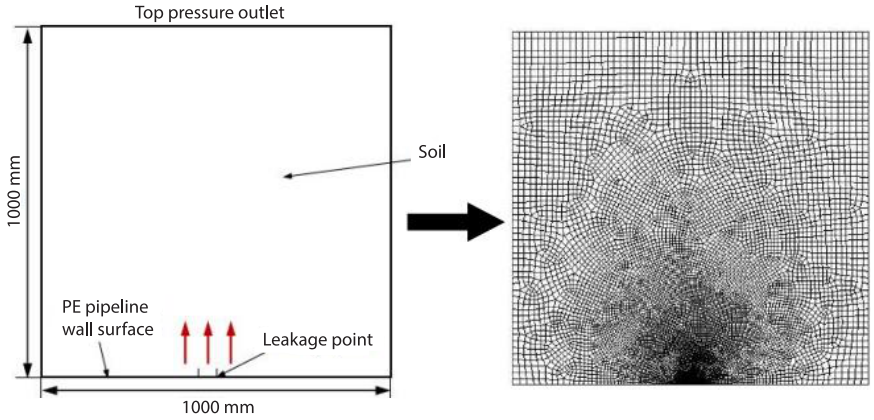

Figure 3. Simplified physical model of buried pipe-line leakage outflow field

Figure 3 shows the diffusion area of natural gas injected from the leak hole to the soil using a 1000 ×1000 mm square 2-D model, *i.e.*, the leak outflow field model, and the soil material was set to simulate the buried pipe-line. The leak was set as the velocity outlet, and the outlets on the left, top, and right sides of the square were all pressure outlets. Similarly, the simulation results of $1 \cdot 10^5$, $3 \cdot 10^5$, and $4 \cdot 10^5$ were compared and found that no significant change in the leakage velocity at the grid number close to $4 \cdot 10^5$. Therefore, the number of meshes is chosen as 394693.

The leaking natural gas dispersion can be regarded as free jet, and the pipe-line leakage process follows the three conservation laws of the flow field above the continuity equation, the Navier-Stokes (N-S) equation, and the energy equation, and follows the turbulence model equation and fundamental equation of a sound wave [14, 15]:

$$\frac{\partial^2 P}{\partial x^2} = \frac{1}{c_0^2}\frac{\partial^2 P}{\partial t^2} \tag{1}$$

$$\nabla^2 P = \frac{1}{c^2}\frac{\partial^2 P}{\partial t^2}$$

$$\nabla^2 \rho = \frac{1}{c^2}\frac{\partial^2 \rho}{\partial t^2} \tag{2}$$

$$\nabla^2 \varphi = \frac{1}{c^2}\frac{\partial^2 \varphi}{\partial t^2}$$

where P is the sound pressure, c_0 – the speed of sound, ∇^2 – the Laplace operator, $\nabla^2 P$ – the second-order derivative of the sound pressure with respect to the spatial position variable, ρ – the density perturbation, and φ – the potential function.

The Lighthill equation is derived from the N-S equation, and Lighthill proposes to use the theoretical model of classical acoustics to study hydrodynamic sound sources for the study of jet noise, *i.e.*, the description of the jet source using the point source approach. The continuity equation and momentum equation obtained using the summation convention is, respectively:

$$\frac{\partial \rho}{\partial t} + \frac{\partial(\rho v_i)}{\partial x_i} = 0 \tag{3}$$

$$\rho\left(\frac{\partial v_i}{\partial t} + v_j \frac{\partial v_i}{\partial x_i}\right) = -\frac{\partial P}{\partial x_i} + \frac{\partial e_{ij}}{\partial x_j} \tag{4}$$

$$e_{ij} = \mu\left(\frac{\partial v_i}{\partial x_j} + \frac{\partial v_j}{\partial x_i} - \frac{2}{3}\delta_{ij}\frac{\partial v_k}{\partial x_k}\right) \tag{5}$$

where v_i is the velocity in x-,y-, and z-directions, e_{ij} – the (i, j) component of the viscous stress tensor, μ – the hydrodynamic viscosity, and δ_{ij} – the Kronecker symbol. Based on the continuity equation and momentum equation, the Lighthill basic equation is obtained as:

$$\frac{\partial^2 \rho}{\partial t^2} - c_0^2 \nabla^2 \rho = \frac{\partial^2 T_{ij}}{\partial x_i \partial x_j} \tag{6}$$

where T_{ij} is the Lighthill turbulence stress tensor,

$$T_{ij} = \rho v_i v_j + \delta_{ij}\left[(P - P_0) - c_0^2(\rho - \rho_0)\right] - e_{ij}$$

Physical modelling and numerical parameter settings

Table 1 shows information about the boundary conditions, and the details of parameter settings and properties of the soil are shown in tab. 2.

The pressure-based solver is chosen, depending on the numerical requirements and characteristics, the FLUENT simulation is divided into two parts: steady-state simulation and transient simulation. The steady-state turbulence model used the pressure-based second-order implicit SIMPLE algorithm and the standard k-ε model, and the transient turbulence model used the FLUENT acoustic model and the large eddy simulation model of vortex. Using the species transport model, the components are defined as methane-air. Since most of the natural gas is CH_4, only CH_4 (mass fraction of 95%) and air (mass fraction of 5%) is selected

for the material composition. The temperature is 300 K, and the pipe-line pressure is set to 0.2 MPa, 0.4 MPa, and 0.8 MPa, to the Chinese town gas design code, and the leak hole sizes are set to 1 mm, 2 mm, and 3 mm to simulate the early stage of leakage.

Table 1. Details of boundary conditions

Boundary location	Boundary type
Pipe inlet	Pressure inlet
Pipe outlet	Pressure outlet
Leakage hole in the pipe-line	Pressure outlet
Surface of the pipe	Wall
Leakage hole in the outflow field model	Velocity outlet
Soil	Interior
Soil boundary (top)	Pressure outlet
Soil boundary (left and right)	Pressure outlet

Table 2. Details of parameter settings and properties of the soil

Related parameters	Value
Leak hole sizes	1 mm, 2 mm, 3 mm
Pipe-line pressure	0.2 MPa, 0.4 MPa, 0.8 MPa
Porosity of soil	0.45
Heat capacity	732.7 J/kgK
Density	2650 kg/m^3
Conductivity	2.9 W/mK
Viscous drag coefficient	$1.96 \cdot 10^{11}$
Inertia drag coefficient	$2.15 \cdot 10^{05}$

Because a large number of complex factors are included, the numerical modelling in a buried gas natural polyethylene pipe-line needs sensible simplification and hypothesis. The following conditions should be assumed in this study:

– The gas in the pipe-line is uniformly mixed, and the pipe-lines provide a continuous and smooth source of gas.
– The heat loss at the wall surface can be ignored and the wall surface is set as a heat-insulating wall, the heat transfer coefficient in the pipe is ignored.
– Without considering the coupling effect between the space wall and the gas-flow.
– The soil is considered to be a porous material that had consistent physical data, including specific heat, thermal conductivity, and an isotropic porosity, *i.e.*, the same resistance in all directions.

Simulation results and analysis

Analysis of pipe-line leakage flow field

Figure 4 shows the flow velocity distribution along the leak hole in the natural gas pipe-line. Enlarged at the leak hole, it can be seen that there was a large velocity gradient of natural gas at the connection between the leak hole and the pipe, which reached the maximum value at the end of the leak hole. The reason is that the pressure difference between the inside

and outside of the pipe caused the original flow state to change, and the intense interaction between the leak hole and the nearby pipe wall and fluid destabilized the overall movement of the fluid in the pipe. The gas in the pipe increased sharply in the direction of the leak hole to gain more kinetic energy and was ejected from the leak hole.

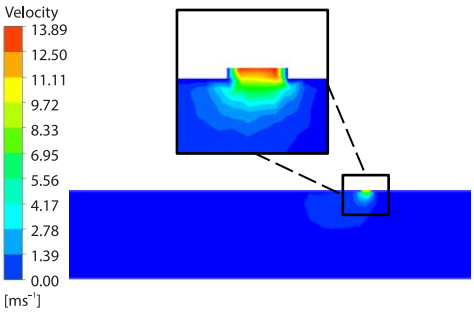

Figure 4. Velocity contour of pipe-line at 0.2 MPa with a 3 mm leakage hole

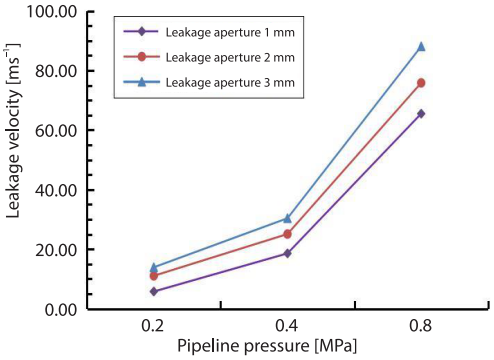

Figure 5. Leakage velocity of internal flow field under different condition

To further analyze the effect of pipe pressure on the leakage velocity of the pipe, the maximum leakage velocities corresponding to the nine operating conditions were plotted on a line as shown in fig. 5. It can be seen that the maximum gas leakage velocity increased with the increase in pipe-line pressure, indicating that the larger the pressure difference between the inside and outside led to the more intense interaction between the leak hole and the nearby tube wall and fluid, thus, the fluid in the tube along the leak hole direction increased in velocity. The expansion of the leak hole size also extended the area of the leak hole and gas, and the maximum gas leak velocity increased.

Figure 6 shows the velocity of natural gas still increased after diffusion from the leak hole to the soil at high speed, and the maximum velocity increased along the direction of the leak hole and appeared at the maximum directly above the leak hole, but the increase was very small. In addition, the peak of the velocity graph was the maximum velocity of gas leakage under the corresponding working conditions in fig. 7, and the flow field of the leak hole had an asymmetric fan-shaped structure distribution. The reason for the aforementioned phenomenon was that the pore resistance inhibits the diffusion of gas, which reduced the increment of flow velocity; and the leakage velocity then decreased rapidly with a large gradient.

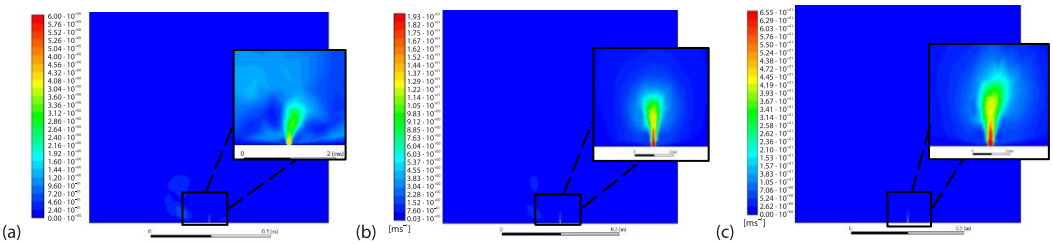

Figure 6. Gas velocity contour under different pipe pressure with 1 mm leakage hole; (a) pipe-line pressure 0.2 MPa, (b) pipe-line pressure 0.4 MPa, and (c) pipe-line pressure 0.8 MPa

In summary, the change of flow field caused by the pipe-line leakage was mainly in the leakage hole and its nearby locations. When the pipe-line leakage occurred, the leakage hole

flow field was an asymmetric fan-shaped structure, that is, the maximum velocity of gas leakage was reached at and near the outlet of the leakage hole, and the maximum flow velocity of the gas leakage increased with the increase in the leakage hole diameter. The flow field indicated shows that the change of the flow field inside and outside the polyethylene pipe due to the natural gas leakage process was the basic premise of fluid-sounding and pneumatic noise generation.

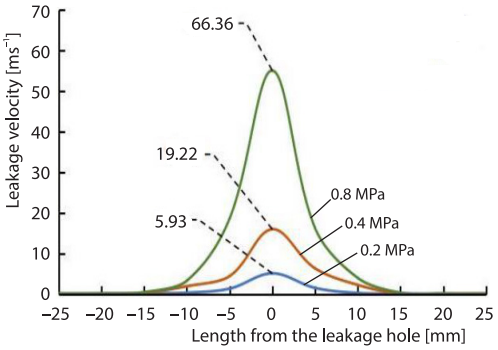

Figure 7. Leakage velocity curves of parallel pipe-line axis

Analysis of the sound pressure level of pipe leakage

Corresponding to the flow field, the leakage sound field was studied by dividing it into internal and external sound fields. The sound power level refers to the total energy magnitude generated by the propagation of sound waves radiating within a fixed unit, fig. 8 shows the sound power level distribution of the pipe-line with a pipe pressure of 0.2 MPa and leak hole diameter of 2 mm. In and around the leak hole was the main distribution area of the sound power sound source generated by the leak, the range is smaller in the pipe, and the maximum value appeared at the point where the pipe meets the leak hole.

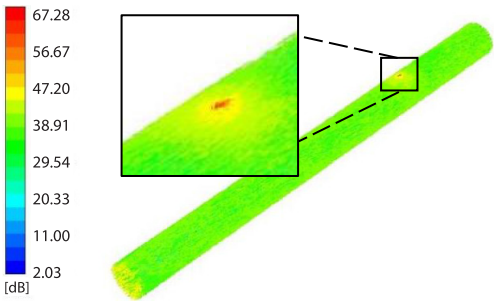

Figure 8. The sound power level contour at 0.2 MPa with 2 mm leakage hole

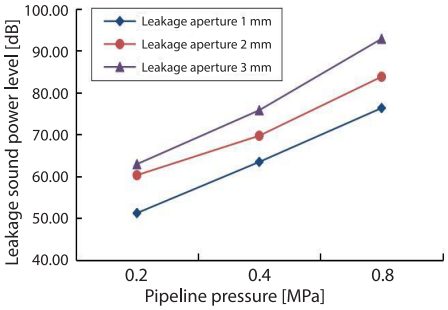

Figure 9. Maximum sound power level diagram of internal field leakage

The line graph of the leakage sound power level under each working condition is plotted in fig. 9. Different pipe pressures had different effects on the leakage sound power level, with the increase in pipe pressure, the maximum leakage sound power level also increased. In addition, with the increase in the leakage orifice diameter, the maximum leakage sound power level also increased in a positive correlation.

The sound field outside the pipe leakage was studied and analyzed, and the sound power clouds of the leakage field for a leakage aperture of 1 mm are shown in fig. 10. Compared with the infield simulation, the maximum sound power level slightly increased. With the increase in pipe pressure, the maximum sound power level of the external leakage increased, and the distribution range of the sound power level cloud was expanded. Figure 11 shows the sound power clouds in the external field at the pipe-line pressure of 0.2 MPa, with the increase in the leak hole size, the sound power level distribution range was expanded. The sound power level clouds, and the sound power level clouds of the external field of the leakage are asymmet-

rically fan-shaped, and the maximum value appeared at the leakage hole and the soil near the leakage hole. The sound power level decayed rapidly in a gradient after spreading to the soil. Unlike the velocity cloud distribution in the external field, the maximum value of sound power level did not appear in the middle of the leak hole, but on both sides of the leak hole. It means that the leaking natural gas has a large kinetic energy when passing through the leak hole at high speed, and a strong friction and collision effect occurs between the hole wall, thus, the greater aerodynamic noise was generated here, and the sound field here had high energy. This also provided the theoretical basis for the subsequent experimental arrangement of sensors.

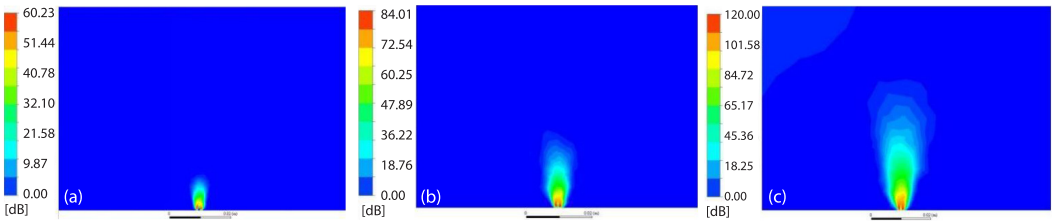

Figure 10. External sound power level contour under different pressures; (a) pipe-line pressure 0.2 MPa, (b) pipe-line pressure 0.4 MPa, and (c) pipe-line pressure 0.8 MPa

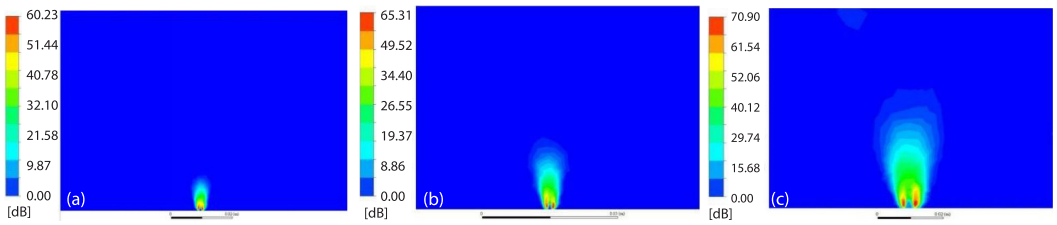

Figure 11. External sound power level contours for different leakage apertures; (a) leakage aperture 1 mm, (b) leakage aperture 2 mm, and (c) leakage aperture 3 mm

The sound pressure level is used to represent the size of the sound, which can visually reflect the change of sound field and energy at the leakage hole, so the frequency domain characteristics of the sound pressure level of the leak source were analyzed. The maximum value of the sound pressure level appeared in the low frequency band from 0-25 Hz, as the frequency of sound waves along the leaky pipe increased, the sound pressure level gradually started to decay, and the trend became steeper and slower. High pressure leaks have more kinetic energy, and the interaction with the pipe wall was more intense and obvious, so the sound pressure level of the sound field generated by high pipe-pressure leaks was larger than the value at low pressure. In addition, the sound pressure level generated by the large leak aperture leakage was also higher, because the increase in aperture diameter created the leak hole wall area and exhibited more intense interaction with the surrounding pipe wall. The simulated spectrum plots will be shown in next section in comparison with the experimental results.

In summary, the change in pipe pressure and leakage orifice diameter affected the change in the flow field and gas-flow velocity of the leakage pipe-line, which affected the sound field. The leakage noise energy increased with the increase in pipe pressure and leakage orifice diameter, and the leakage noise energy was closely related to the pulsating pressure change, flow field density, velocity gradient, and other parameters.

Experimental verification and discussion

Details of the experiment device

The polyethylene pipe-line leakage detection platform was built for the experiment to verify the simulation results and the feasibility of the sound source characteristic-based leak detection method, as shown in fig. 12. The experimental natural gas polyethylene pipe diameter was 80 mm, wall thickness was 5 mm, and burial depth was 800 mm. Considering the operability of the experiment, a ball valve was used to simulate the leakage hole, and the opening degree was calculated to control the leakage hole size. A low frequency sound pressure level sensor with a measurement range of 30-130 dB.

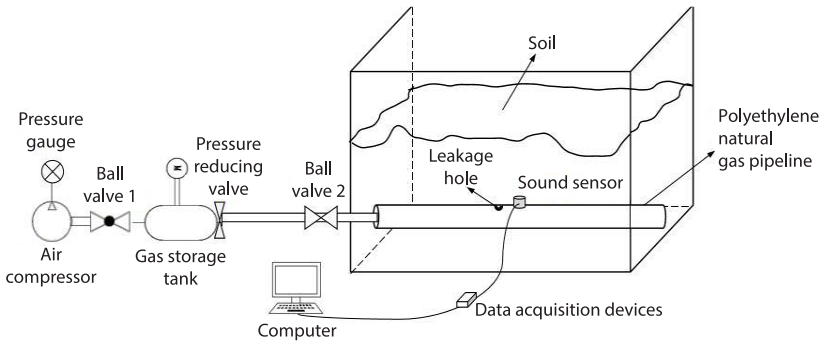

Figure 12. Experimental diagram of leakage of natural gas polyethylene pipe-line

Before the experiment, the soil porosity was measured using the ring knife method. The ring knife method is a simple and easy method to measure soil capacity. A known steel ring knife or cylinder of a certain mass and volume is used to truncate the soil in its natural state, obtain a soil sample, calculate the weight of dry soil per unit volume by some series of weighing and measuring, get the soil capacity and calculate the soil porosity. Three groups of soils were sampled in the vicinity of the buried pipes and the measurements yielded an average porosity of 0.452. Then checked the air tightness of the test device, turned on the power supply, and started the air compressor, when the pressure in the storage tank reached the requirements, opened the outlet valve. Placed the sensor at the leak hole 5 mm, opened the gas inlet valve, and let the gas enter the pipe-line. The pressure regulator should be adjusted from high to low, with the pressure being 0.8 MPa, followed by 0.4 MPa, and 0.2 MPa. When the gas in the pipe was stable, the instantaneous flow rate and the changes in sound pressure level parameters under this leakage condition were collected and recorded in real-time. Closed the inlet main valve, adjusted the opening degree and angle of the ball valve, changed the leakage orifice diameter (1-3 mm), and repeated the previous experiment. Collected data corresponding to three types of pipe-line pressure for each leakage hole size, and after completion, waited for the pressure gas to stabilize and then closed the leak valve.

Experimental and simulation results and analysis

Firstly, the instantaneous maximum leakage flow of natural gas is measured and the corresponding maximum leakage velocity is calculated. The data are shown in tab. 3, and the results show that the larger the leak aperture and pressure, the larger the instantaneous leak volume and the maximum gas leak rate. It is known that the larger the aperture and pressure are, the easier the soil uplift zone or crater will be formed, in addition, the more gas leaks into the soil cavity, the shorter the time within the explosion limit [16-18]. This also proves the neces-

sity and importance of rapid detection of pipe-line leaks based on sound source characteristics in the initial stage.

Table 3. Comparative record of simulation and experimental data

Leakage conditions and data recording		0.2 MPa	0.4 MPa	0.8 MPa
1 mm	Experimental value [ms^{-1}]	5.50	15.51	58.42
	Simulation value [ms^{-1}]	5.90	19.22	66.36
	Relative error	6.78%	19.30%	11.97%
2 mm	Experimental value [ms^{-}1]	9.62	22.16	70.41
	Simulation value [ms^{-1}]	11.19	25.37	76.57
	Relative error	14.03%	12.65%	8.04%
3 mm	Experimental value [ms^{-1}]	10.96	27.83	81.00
	Simulation value [ms^{-1}]	14.54	30.67	89.76
	Relative error	24.62%	9.26%	9.76%

The sound pressure frequency characteristics and sound pressure level values were measured and subsequently processed for calculation. Then, the processed experimental sound pressure spectrogram was compared with the simulated results as shown in fig. 13. The experimentally obtained sound pressure spectra of the natural gas pipe-line leaks were consistent with the simulation results showing the decay trend, and the experimental results better corroborated the previous FLUENT simulation of the sound source characteristics of leaks. This was considered to be a more accurate measurement.

The maximum sound pressure level and the average sound pressure level of the leak were calculated based on the obtained sound pressure spectrograms. Figure 14 shows the comparison curves of the average value of the sound pressure level with the change in pipe pressure and leakage aperture diameter under the experimental and simulation cases, respectively. Figure 15 shows the comparison curves of the maximum value of the sound pressure level. It can be seen that the experimental results and the simulation analysis had the same variation pattern, which indicated that there were indeed obvious changes in the sound field and source characteristics when the buried natural gas polyethylene pipe-line was leaking.

The following reasons are summarized for the errors: there is power loss in the working process of the experimental equipment and instruments, the length of the natural gas pipeline is limited, and the model and parameters set in the simulation are ideal and keep the constant value without disturbance, such as the soil is the ideal medium. However, when leakage occurs, the degree of soil looseness and porosity are not uniform, violent friction exists on the wall of the pipe, natural gas leakage is accompanied by heat exchange*, etc.* The aforementioned analysis explains why there is a general error, and the experimental values are smaller than the simulated values.

Overall, the experimentally measured leakage velocity, sound pressure spectrograms, and sound pressure level eigenvalues of the pipe-line were verified by cross-comparison with simulation results, the data is within the error range, which shows that the numerical simulation results are consistent with the experimental results and confirm the reliability of the numerical calculation results. The accuracy of the model is verified, illustrating the theoretical feasibility of conducting leak detection of buried natural gas polyethylene pipe-lines based on the sound source characteristic principle.

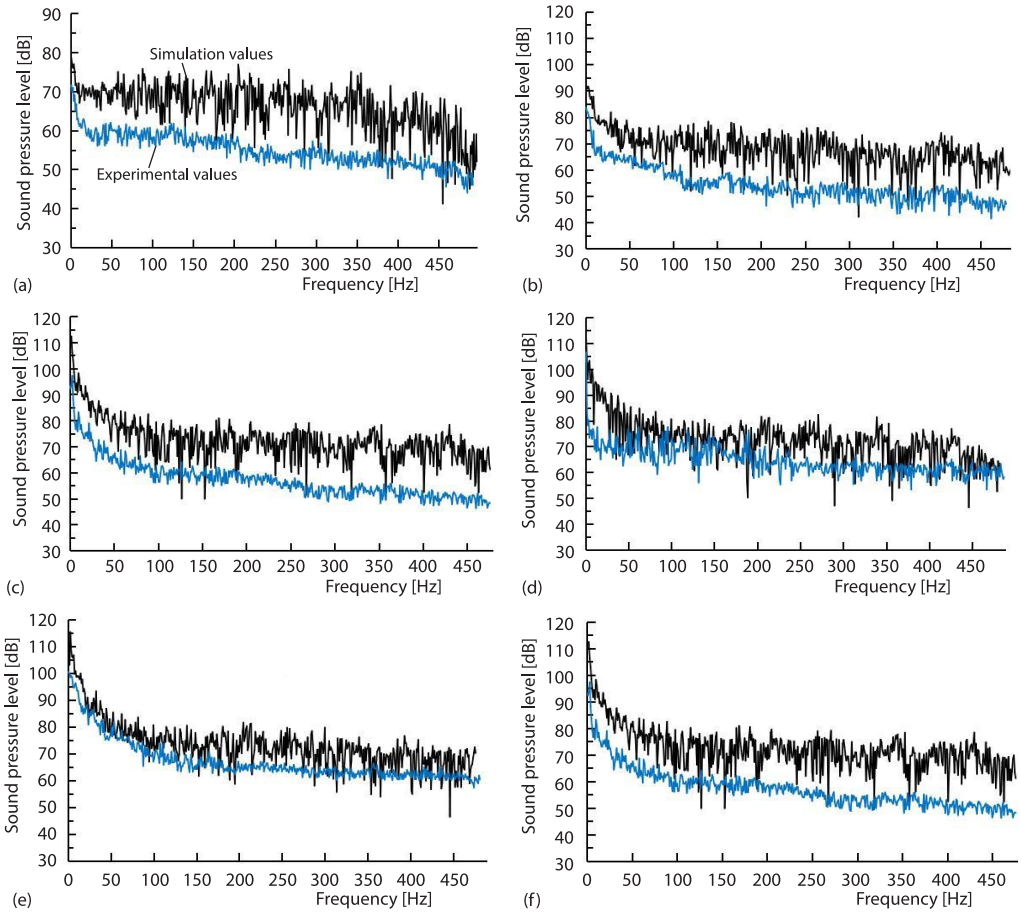

Figure 13. Comparison of sound pressure spectrum between experiment and simulation results; (a) pipe-line pressure 0.2 MPa, (b) pipe-line pressure 0.4 MPa, (c) pipe-line pressure 0.8 MPa, (d) leakage aperture 3 mm, (e) leakage aperture 2 mm, and (f) leakage aperture 1 mm

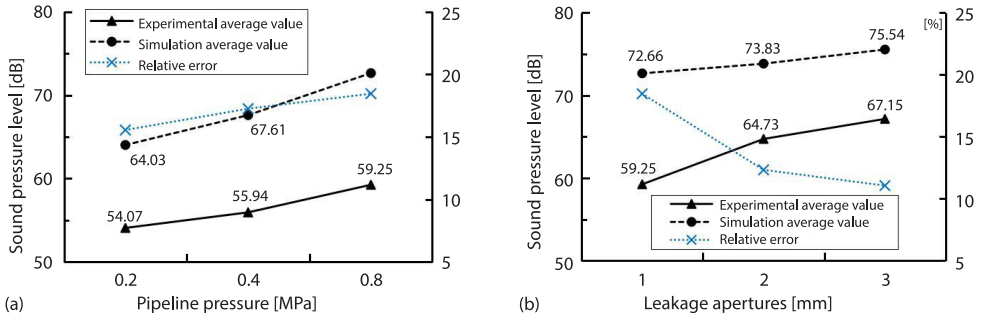

Figure 14. Comparison curves of average sound pressure level; (a) under different pipe pressures and (b) with different leakage apertures

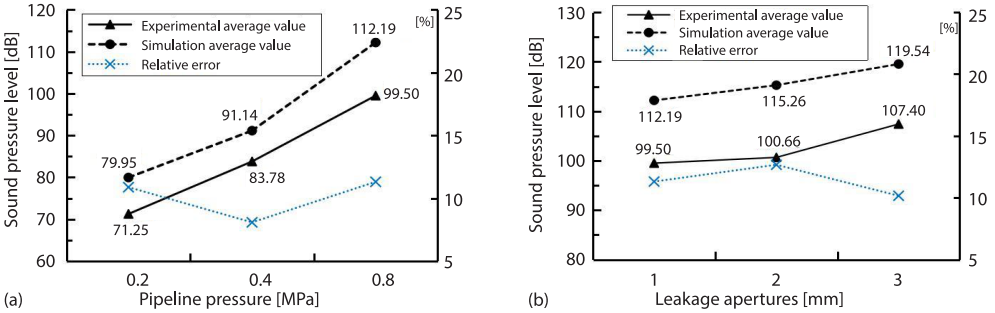

Figure 15. Comparison curves of maximum sound pressure level; (a) under different pipe pressures and (b) with different leakage apertures

Conclusions

The larger the leak aperture and pressure are, the greater the instantaneous leakage is. The sound sources generated by the pipe-line leakage are mainly distributed in and around the leakage hole and the maximum value is at the connection between the pipe-line and the leakage hole. There is a regular variation of the sound power level at different pressures and different leakage hole diameters. Analysis of the spectrum of the sound pressure level at the leak hole indicates the average and maximum value of the sound pressure level both increase with the increase in pipe pressure and leak hole diameter. Sound waves below the 25 Hz band have higher sound pressure level value and energy.

The polyethylene pipe-line leakage detection platform was built, and the simulation data matched well with the experimental data, which verified the accuracy of the simulation model. This confirmed the simulation analysis results and laws and provided a theoretical basis for the buried natural gas polyethylene pipe-line leak detection method based on sound source characteristics.

Acknowledgment

This work was supported by the Natural Science Foundation of China (Grant No. 51871206).

Nomenclature

c – speed of fluid, [ms^{-1}]
c_0 – speed of sound, [ms^{-1}]
e_{ij} – component of viscous stress tensor
P – sound pressure, [Pa]
$\nabla^2 P$ – second-order derivative of the sound pressure with respect to the spatial position variable
T_{ij} – Lighthill turbulence stress tensor
t – time, [s]
v_i – velocity in x-, y-, and z-directions, [ms^{-1}]

Greek symbols

μ – hydrodynamic viscosity, [Pa·s]
δ_{ij} – Kronecker symbol
ρ – density perturbation
φ – potential function
∇^2 – Laplace operator

References

[1] Chen, S., *et al.*, Simulation and Analysis of Buried Pipe Heat Transfer Performance under Leakage State, *Thermal Science*, *25* (2021), 2A, pp. 859-868
[2] Wang, L. L., *et al*., Numerical Investigation of Gas Dispersion Effect on Laser Detection of Natural Gas Pipe-Line Leak, *Thermal Science*, *22* (2018), 2, pp. 607-615
[3] Jia, Z. W., *et al.*, Propagation Law of Flame in a Pipe-line Produced in Gas Explosion Numerical Analysis and Experimental Verification, *Thermal Science*, *25* (2021), 3B, pp. 2199-2204

[4] Korlapati, N. V., *et al*., Review and Analysis of Pipe-Line Leak Detection Methods, *Journal of Pipe-line Science and Engineering*, *2* (2022), 4, 100074
[5] Meng, L. Y., et al., Experimental study on leak detection and location for gas pipe-line based on acoustic Method, *Journal of Loss Prevention in the Process Industries*, *25* (2011), 1, pp. 90-102
[6] Li, Y. B., *et al*., Influence of Leakage Hole Shape on the Leakage Sound Source Characteristics of Gas Pipe-Line, *China Measurement and Test*, *46* (2020), 11, pp. 139-145
[7] Xiao, R., *et al*., Experimental Investigation on Characteristics of Leak Noise in Gas Pipe-Line Systems, *Journal of Pipe-line Systems Engineering and Practice*, *13* (2022), 1
[8] Ye, Y. C., *et al*., Characteristics and Variation Rules of Acoustic Source of Gas Pipe-Line Leaks, *Natural Gas Industry*, *36* (2016), 8, pp. 124-131
[9] Ali, S., *et al.*, Effect of Leak Geometry on Water Characteristics Inside Pipes, *Sustainability*, *14* (2022), 9, pp. 5224-5245
[10] Oosterkamp, A., *et al*., Effect of the Choice of Boundary Conditions on Modelling Ambient to Soil Heat Transfer Near a Buried Pipe-Line, *Applied Thermal Engineering*, *100* (2016), May, pp. 367-377
[11] Zhu, Q., Numerical Simulation and Application of Soil Temperature Field around Buried Thermal Pipe-Line (in Chinese), M. Sc. thesis, Xi'an Shiyou University, Xi'an, China, 2017
[12] Dehdarinejad, M., *et al*., Experimental and Numerical Simulation on Buried Hot Fuel Oil Pipe-Lines in Three Modes Flow Regime Considering Temperature Loss during a Shutdown, *Thermal Science*, *25* (2021), 1B, pp. 757-766
[13] Xiao, R., Simulation Study on Leakage and Diffusion of Buried Gas Pipe-Line in Soil (in Chinese), M. Sc. thesis, Harbin Institute of Technology, Harbin, China, 2019
[14] Yu, Z., *et al*., Study on Acoustic Detection Method of Gas Pipe-Line Leakage, IOP Conference Series, *Earth and Environmental Science*, *558* (2020), 022032
[15] Wang, C., *et a*l., Study on Acoustic Source Characteristics of Distributed Optical Fiber Acoustic Wave Monitoring Buried Natural Gas Pipe-Line Leakage, *E3S Web of Conferences*, *252* (2021), Apr., pp. 43-48
[16] Yan, Y. T., *et al*., Experimental Study of Methane Diffusion in Soil For an Underground Gas Pipe Leak, *Journal of Natural Gas Science and Engineering*, *27* (2015), pp. 82-89
[17] Caroline, B., *et al*., Experimental Study and Modelling of the Consequences of Small Leaks on Buried Transmission Gas Pipe-Line, *Journal of Loss Prevention in the Process Industries*, *55* (2018), pp. 303-312
[18] Xia, J. B., *et al*., Experimental Research on Gas Leakage Flow from Buried Gas Pipe-lines and Its Diffusion Law, *GAS and HEAT*, *36* (2016), 6, pp. 36-42

Paper submitted: March 13, 2023
Paper revised: April 9, 2023
Paper accepted: April 11, 2023